ORIGINAL RESEARCH PAPER

# Buckling of Doubly Clamped Nano-Actuators in General form Through Spectral Meshless Radial Point Interpolation (SMRPI)

***Hedayat Fatahi [1]*, Elyas Shivanian [2], S. J. Hosseini Ghoncheh [3, 4]***

[1] *Department of Mathematics, Baneh Branch, Islamic Azad University, Baneh, Iran*
[2] *Department of Applied Mathematics, Imam Khomeini International University, Qazvin, Iran*
[3] *Young Researchers & Elite Club, Pharmaceutical Sciences Branch, Islamic Azad University, Tehran, Iran*
[4] *Department of Basic Sciences, Pharmaceutical Sciences Branch, Islamic Azad University (IAUPS), Tehran, Iran*

Received: 2017-04-07 Accepted: 2017-05-08 Published: 2017-06-25

**ABSTRACT**
The present paper is devoted to the development of a kind of spectral meshless radial point interpolation (SMRPI) technique in order to obtain a reliable approximate solution for buckling of nano-actuators subject to different nonlinear forces. To end this aim, a general type of the governing equation for nano-actuators, containing integro-differential terms and nonlinear forces is considered. This general type for the nano-actuators is a non-linear fourth-order Fredholm integro-differential boundary value problem. The point interpolation method with the help of radial basis functions is used to construct shape functions which play as basis functions in the frame of SMRPI. In the current work, the thin plate splines (TPSs) are used as radial basis functions. This numerical based technique enables us to overcome all kind of nonlinearities in the mentioned boundary value problem and then to obtain fast convergent solution. Thus, it can facilitate the design of nano-actuators.

**Keywords:** *Nano-actuator, Spectral meshless radial point interpolation (SMRPI) method; Radial basis function; Fredholm integral equation.*


**How to cite this article**
*Fatahi H, Shivanian E, Hosseini Ghoncheh SJ. Buckling of Doubly Clamped Nano-Actuators in General form Through Spectral Meshless Radial Point Interpolation (SMRPI). J. Nanoanalysis., 2017; 4(1): 76-84.* DOI: 10.22034/jna.2017.01.009

## INTRODUCTION AND MATHEMATICAL MODEL

In fact, a basic inevitable part of many nano/micro electro mechanical systems is a nano/micro actuator. The actuator consists of a beam suspended over a substrate in nano/micro mechanical actuators or in nano/micro mechanical sensors. Electrostatic field is induced by imposing a voltage difference between the the substrate and beam, and therefore, the electrostatic forces captivate the beam into the substrate [18]. Furthermore, beam and substrate acts as a capacitor, where the motion of the beam can be detected by the capacitive change as a signal [5]. The nano-actuators are subject to different inherently nonlinear forces such as dielectric effects, fringing field effects, van der Waals attractions and Casimir force [42, 39, 25]. On the other hand, the axial forces in the clamped-clamped type of nano-actuators is consequential matter and should be considered. The presence of such axial forces causes an integro-differential term to the governing equation of the nano-actuators [2, 3, 9]. As a conclusion, since the actuators are manufactured in packs as many as thousands for sensors and billions for chipsets in the applications of nano-/micro-actuators

* Corresponding Author Email: fatahi_iau@yahoo.com, Tel: +98 (918)3746515

then, presenting more accurate technique in order to analyze nano/micro structures including these actuators is of interest to the researchers.

Consider the following general governing equation of a nano-actuator beam augmented to boundary conditions, including the effect of axial loads and all different types of nonlinear forces [18]

$$\frac{\mathrm{d}^4u}{\mathrm{d}x^4}-\left(\eta\int_0^1\left(\frac{\mathrm{d}u}{\mathrm{d}x}\right)^2\mathrm{d}x+P\right)\frac{\mathrm{d}^2u}{\mathrm{d}x^2}+\frac{\alpha}{u^\zeta}+\frac{\beta}{(\kappa+u)^2}+\frac{\gamma}{u}=0,\quad x\in[0,1],\qquad(1)$$

$$u(0)=u(1)=1,u'(0)=u'(1)=0,\qquad(2)$$

where all variables and parameters are in the non-dimensional form, $u$ is the deflection of the beam and $x$ is the length of the beam. $P$ and $\eta$ represent the effect of axial forces, $\beta$ denotes the effect of the external applied voltage, $\kappa$ represents the effect of a dielectric layer, $\gamma$ represents the fringing field or the capillary effect, $\zeta$ is an integer positive number and the concept of the parameter $\alpha$ depends on the value of $\zeta$ i.e. in the case of $\zeta=3$, $\alpha$ denotes the van der Waals effects, and in the case of $\zeta=4$, $\alpha$ denotes the Casimir effect.

The boundary value problem (1)-(2) has been studied in some special cases. In [3] authors considered term including $P$. Authors of [42, 3, 9] studied on the force $\eta\int_0^1\left(\frac{\mathrm{d}u}{\mathrm{d}x}\right)^2\mathrm{d}x$. In [26, 17], it has been the term containing $\beta$. Authors in [17, 23, 29] considered the force $\gamma$. Also, the nonlinear forces term $\frac{\alpha}{u^3}$ in [39, 23], the nonlinear forces term $\frac{\alpha}{u^4}$ in [25, 29, 24] and $\kappa$ in [42] have been used. Furthermore, the boundary value problem (1)-(2) in the general form has been analyzed by a modification of Adomian decomposition method (ADM) namely Duan-Rach Adomian decomposition method [18]. Adomian decomposition method and its modification are some kind of semi-analytical method [4, 27, 41]. Although many authors find that the ADM requires less computational work than traditional approaches but they do have some disadvantages, however. The first is that the method gives a series solution which must be truncated for practical applications. In addition, the rate and region of convergence are potential shortcomings. According to Jiao et al. [22], "although the series can be rapidly convergent in a very small region, it has very slow convergence rate in the wider region...and the truncated series solution is an inaccurate solution in that region, which will greatly restrict the application area of the method."

Meshless methods have attracted much attention in recent years [15, 14]. There are various types of meshless techniques, for example, meshless techniques based on weak forms such as the element-free Galerkin (EFG) method [13, 30, 16], diffuse element method [28], meshless local radial point interpolation method [37, 33], meshless local Petrov-Galerkin method [11, 38, 31] and including their developments; meshless techniques based on collocation techniques (strong forms) such as the meshless collocation technique based on radial basis functions (RBFs) and finally meshless techniques based on the combination of weak forms and collocation technique [8, 32, 20, 6, 35, 10, 40, 1, 19, 21, 7].

Shivanian [34, 36] proposed a kind of spectral meshless radial point interpolation (SMRPI) method which is based on meshless methods and benefits from spectral collocation ideas. In SMRPI technique, the point interpolation method with the help of those radial basis functions, which were free of shape parameter, has been proposed to construct shape functions which have Kronecker delta function property. Based on spectral methods, evaluation of high order derivatives of given differential equation is not difi¬ cult by constructing and using operational matrices. Our aim in this work is the development of SMRPI method to obtain the solution of the boundary value problem (1)-(2). It will be seen the method with high performance, while is numerical based, can easily overcome the all kind of nonlinear terms and obtain more accurate approximate solutions in a fast way.

Meshless methods have attracted much attention in recent years [1,6-8,10-11,13-16,19-21,28,30-33,35,37-38,40]. One of the very useful and easy to apply among meshless methods has been improved by Shivanian [34, 36] which is a kind of spectral meshless radial point interpolation (SMRPI) method. Our aim in this work is the development of this technique to obtain the solution of the boundary value problem (1)-(2). It will be seen the method with high performance, while is numerical based, can easily overcome the all kind of nonlinear terms and obtain more accurate approximate solutions in a fast way.

*Proposed Method*

We concentrate on how to obtain the shape functions as basis function for SMRPI approach in current section. Since we use the radial basis function of conditionally positive definite to build the shape functions, remember the following definition and theorem from [12].

*Definition*

Suppose that function $\phi:\mathbb{R}^d\to\mathbb{R}$ is continuous, it is called conditionally positive semi-definite of order $m$ if, for all $N\in\mathbb{N}_o$, all

pairwise distinct centers $x_1,\ldots,x_N \in \mathbb{R}^d$, and all $c=[c_1,\ldots,c_N]^{tr} \in C^N$ are such that

$$\sum_{j=1}^{N} c_j p(x_j) = 0$$

for all complex-valued polynomials of degree less than $m$, the quadratic form

$$\sum_{j=1}^{N}\sum_{k=1}^{N} c_j \bar{c}_k \varphi(x_j - x_k)$$

is positive or zero. Furthermore, the function $\phi$ is called conditionally positive definite of order $m$ if the above quadratic formula is positive, unless $c$ is zero.

*Theorem (Micchelli)*

Suppose that $\phi \in C[0,\infty) \cap C^{\infty}(0,\infty)$ is given. The function $\varphi = \phi(\|\cdot\|^2)$ is conditionally positive semi-definite of order $N \in \mathbb{N}_0$ on $\mathbb{R}^d$ iff $(-1)^m \phi^{(m)}$ is completely monotone on $(0,\infty)$.

Now, one can find easily as many as conditionally positive definite functions by using this theorem. For an example, the thin-plate or surface splines $\phi(r) = (-1)^{k+1} r^{2k} \log(r)$ are of order $m = k+1$ on $\mathbb{R}^d$. Assume that the function $u(x)$ is continuous on a domain $\Omega \subset \mathbb{R}^d$, $d = 1,2$, where it is constructed using a set of nodal points called field nodes. The $u(x)$ at arbitrary considered point $x$ is represented approximately as

$$u(x) = \sum_{i=1}^{n} R_i(x) a_i + \sum_{i=1}^{np} P_j(x) b_j = R^{tr}(x) a + P^{tr}(x) b, \quad (3)$$

Where it constituted of the number of $n$, radial basis function (RBF) $R_i(x)$ and the number of $np$ monomial $P_j(x)$. The $P_j(x)$ in Eq. (3) is built using Pascal's triangle and a complete basis is usually preferred. The linear basis functions, to construct shape functions, are given by

$$P^{tr}(x) = \{1, x\}, \quad np = 2 \quad (1D),$$

$$P^{tr}(x) = \{1, x, y\}, \quad np = 3 \quad (2D),$$

the quadratic basis forms

$$P^{tr}(x) = \{1, x, x^2\}, \quad np = 3 \quad (1D),$$

$$P^{tr}(x) = \{1, x, y, x^2, y^2, xy\}, \quad np = 6 \quad (2D),$$

and the cubic basis functions are constituted of

$$P^{tr}(x) = \{1, x, x^2, x^3\}, \quad np = 4 \quad (1D),$$

$$P^{tr}(x) = \{1, x, y, x^2, y^2, xy, x^3, y^3, x^2 y, xy^2\}, \quad np = 10 \quad (2D).$$

It is worth-mentioning here that the second part of Eq. (3), i.e. the polynomials, are not necessary when the RBFs are chosen from the category of strictly positive definite radial basis function otherwise they are needed. Therefore, when the TPS is employed for interpolation, the polynomial terms are needed to avoid the singularity. Coefficients $a_i$ and $b_j$ are unknown which should be determined. To discover $a_i$ and $b_j$ in Eq. (3), a so-called support domain is formed for the considered point x, and $n$ field nodes belong to this support domain (a typical support domain is a disk with radius $r_s$). Coefficients $a_i$ and $b_j$ can be determined by enforcing Eq. (3) to be satisfied at these $n$ field nodes in the neighborhood of the considered point $x$. Hence, a linear system of equations is formed corresponding to each nodal point. The resulted system of equations in the matrix form are as follows

$$U_s = R_n a + P_{np} b, \quad (4)$$

in where $U_s$ is a vector as

$$U_s = \{u_1, u_2, u_3, \ldots, u_n\}^{tr}, \quad (5)$$

the RBFs moment matrix is

$$R_n = \begin{pmatrix} R_1(r_1) & R_2(r_1) & \cdots & R_n(r_1) \\ R_1(r_2) & R_2(r_2) & \cdots & R_n(r_2) \\ \vdots & \vdots & \ddots & \vdots \\ R_1(r_n) & R_2(r_n) & \cdots & R_n(r_n) \end{pmatrix}_{n \times n}, \quad (6)$$

and the polynomial moment matrix is

$$P_{np}=\begin{pmatrix}1 & x_1 & y_1 & \cdots & P_{np}(x_1)\\ 1 & x_2 & y_2 & \cdots & P_{np}(x_2)\\ \vdots & \vdots & \vdots & \ddots & \vdots\\ 1 & x_n & y_n & \cdots & P_{np}(x_n)\end{pmatrix}_{n\times np}, \quad (7)$$

Also, the vector of unknown coefficients for RBFs is

$$a^{tr}=\{a_1,a_2,\cdots,a_n\}, \quad (8)$$

and the vector of unknown coefficients for polynomial is

$$b^{tr}=\{b_1,b_2,\cdots,b_{np}\}. \quad (9)$$

Note that in Eq. (6), $r_k$ in $R_i(r_k)$ is in fact distance, i.e.

$$r_k=\sqrt{(x_k-x_i)^2}, \qquad \text{for1D}, \quad (10)$$

$$r_k=\sqrt{(x_k-x_i)^2+(y_k-y_i)^2}, \qquad \text{for2D}. \quad (11)$$

Because in Eq. (3) there are $n+np$ unknown variables, for guarantee uniqueness of approximation, add $np$ condition as follows

$$\sum_{i=1}^{n}P_j(x_i)a_i=P_{np}^{tr}a=0, \quad j=1,2,\cdots,np. \quad (12)$$

Now by combining Eq. (3) and Eq. (12) we obtain the aimed system of linear equations in the matrix shape as:

$$\widetilde{U}_s=\begin{pmatrix}U_s\\ 0\end{pmatrix}=\begin{pmatrix}R_n & P_{np}\\ P_{np}^{tr} & 0\end{pmatrix}\begin{pmatrix}a\\ b\end{pmatrix}=G\,\widetilde{a}, \quad (13)$$

where

$$\widetilde{U}_s^{tr}=\{u_1,u_2,\cdots,u_n,0,0,\cdots,0\}, \quad \widetilde{a}^{tr}=\{a_1,a_2,\cdots,a_n,b_1,b_2,\cdots,b_{np}\}. \quad (14)$$

Solving Eq. (13), we obtain

$$\widetilde{a}=\begin{pmatrix}a\\ b\end{pmatrix}=G^{-1}\widetilde{U}_s. \quad (15)$$

Now by rewrite of Eq. (3) have

$$u(x)=\{R^{tr}(x),P^{tr}(x)\}G^{-1}\widetilde{U}_s=\widetilde{\boldsymbol{\Phi}}^{tr}(x)\widetilde{U}_s, \quad (16)$$

where

$$\widetilde{\boldsymbol{\Phi}}^{tr}(x)=\{R^{tr}(x),P^{tr}(x)\}G^{-1}=\{\varphi_1,\varphi_2,\cdots,\varphi_n,\varphi_{n+1},\varphi_{n+2},\cdots,\varphi_{n+np}\}. \quad (17)$$

We call the first $n$ functions of the above vector function as the RPIM shape functions corresponding to each nodal displacements and we show by the vector $\boldsymbol{\Phi}^{tr}(x)$, that's mean

$$\boldsymbol{\Phi}^{tr}(x)=\{\varphi_1,\varphi_2,\cdots,\varphi_n\}. \quad (18)$$

Now Eq. (16) becomes

$$u(x)=\boldsymbol{\Phi}^{tr}(x)U_s=\sum_{i=1}^{n}\varphi_i(x)u_i. \quad (19)$$

It is consequential matter that the RPIM shape functions enjoy the Kronecker delta function property which is in fact

$$\varphi_i(x_j)=\begin{cases}1 & \text{for i=j,j=1,2,...,n}\\ 0 & \text{for i}\neq\text{j,i,j=1,2,...,n}\end{cases}. \quad (20)$$

This fact is concluded from that they pass

through nodal values. Furthermore, the shape functions have also the property of partitions of unity, i.e.

$$\sum_{i=1}^{n}\varphi_i(x)=1. \tag{21}$$

*Implementation of the SMRPI Method*

At first, some notations on derivatives of shape function are needed to be described then we focus on how to implement the SMRPI for Eq. (1). In the current work, we assume that the number of total nodes covering $\Omega=(\Omega\cup\partial\Omega)$ is $N$. Also, suppose that $n_x$, instead $n$, is the number of field nodes distributed in support domain $\Omega_x$ corresponding to each considered point of interest $x=x$, for 1D, or $x=(x,y)$, for 2D. For example $\Omega_x$ can be a disk cantered at $x$ with radius $r_s$. By rewriting the Eq. (19), we have

$$u(x)=\ddot{\mathbf{O}}^{tr}(x)U_s=\sum_{j=1}^{N}\varphi_j(x)u_j. \tag{22}$$

We know that for each point $x_j$ there exists a shape (basis) function $\varphi_j(x), j=1,2,...,N$, we define $\Omega^c x=\{x_j : x_j\notin\Omega\ x\}$ then it is clear from Eq. (20) that

$$\forall x_j\in\Omega^c x:\varphi_j(x)=0. \tag{23}$$

Now the derivatives of $u(x)$ respect to $x$ and $y$ are

$$\frac{\partial u(x)}{\partial x}=\sum_{j=1}^{N}\frac{\partial\varphi_j(x)}{\partial x}u_j,\quad \frac{\partial u(x)}{\partial y}=\sum_{j=1}^{N}\frac{\partial\varphi_j(x)}{\partial y}u_j, \tag{24}$$

and for high derivatives of $u(x)$

$$\frac{\partial^s u(x)}{\partial x^s}=\sum_{j=1}^{N}\frac{\partial^s\varphi_j(x)}{\partial x^s}u_j,\quad \frac{\partial^s u(x)}{\partial y^s}=\sum_{j=1}^{N}\frac{\partial^s\varphi_j(x)}{\partial y^s}u_j, \tag{25}$$

where $\frac{\partial^s(.)}{\partial x^s}$ and $\frac{\partial^s(.)}{\partial x^s}$ are s'th derivatives with respect to $x$ and $y$. Now, substituting $x=x_i$, or $x=(x_i,y_i)$ in above equations

$$U_x^{(s)}=D^{(s)}xU,\quad U_y^{(s)}=D^{(s)}yU, \tag{26}$$

where

$$U_x^{(s)}=(u_{x_1}^{(s)},u_{x_2}^{(s)},...,u_{x_N}^{(s)})^{tr},\quad U_y^{(s)}=(u_{y_1}^{(s)},u_{y_2}^{(s)},...,u_{y_N}^{(s)})^{tr}, \tag{27}$$

$$D_{x_{ij}}^{(s)}=\frac{\partial^s\varphi_j(x_i)}{\partial x^s},\quad D_{y_{ij}}^{(s)}=\frac{\partial^s\varphi_j(x_i)}{\partial y^s}, \tag{28}$$

and

$$U=(u_1,u_2,...,u_N)^{tr}. \tag{29}$$

It is necessary that we mention $\forall x_j\in\Omega^c x:\partial^s\varphi_j(x)/\partial x^s=\partial^s\varphi_j(x)/\partial y^s=0, s=1,2,...$, due to Eq. (23).

Now, we can state the SMRPI method for Eq. (1), only for 1D, as follows. Replacing approximate Eqs. (22) and (25) into Eq. (1) yields

$$\sum_{j=1}^{N}\frac{\partial^4\varphi_j(x)}{\partial x^4}u_j=\left(\eta\int_0^1\left(\sum_{j=1}^{N}\frac{\partial\varphi_j(x)}{\partial x}u_j\right)^2dx+P\right)\sum_{j=1}^{N}\frac{\partial^2\varphi_j(x)}{\partial x^2}u_j-\frac{\alpha}{u^c}-\frac{\beta}{(\kappa+u)^2}-\frac{\gamma}{u} \tag{30}$$

Now, setting $x=x_i$, $i=1,2,...,N_\Omega$ ($N_\Omega$ is the number of nodal points in $\Omega$) in the latest equation and enjoying the notations (26)-(29) imply

$$\sum_{j=1}^{N}D_{x_{ij}}^{(4)}u_j=\left(\eta\int_0^1\left(\sum_{j=1}^{N}\frac{\partial\varphi_j(x)}{\partial x}u_j\right)^2dx+P\right)\sum_{j=1}^{N}D_{x_{ij}}^{(2)}u_j-\frac{\alpha}{u_i^c}-\frac{\beta}{(\kappa+u_i)^2}-\frac{\gamma}{u_i}. \tag{31}$$

For those nodal points which are put on the boundary $\partial\Omega$ using Eq. (2), we adopt the following relations which come from the original boundary conditions

$$u_1 = 1, \quad u_N = 1, \tag{32}$$

$$\sum_{j=1}^{N} D^{(1)}_{x_{1j}} u_j = 0, \quad \sum_{j=1}^{N} D^{(1)}_{x_{Nj}} u_j = 0. \tag{33}$$

Now, we turn back to Eq. (31), suppose that $u_i, i = 1,2,...,N$ are known already. We have to approximate the integral

$$\int_0^1 \left( \sum_{j=1}^{N} \frac{\partial \varphi_j(x)}{\partial x} u_j \right)^2 \mathrm{d}x .$$

The procedure is to apply two dimensional Gaussian quadrature rule as follows:

$$\int_0^1 \left( \sum_{j=1}^{N} \frac{\partial \varphi_j(x)}{\partial x} u_j \right)^2 \mathrm{d}x = \frac{1}{2} \int_{-1}^{1} \left( \sum_{j=1}^{N} \frac{\partial \varphi_j\left(\frac{1}{2}(x+1)\right)}{\partial x} u_j \right)^2 \mathrm{d}x$$

$$= \frac{1}{2} \sum_{k=1}^{n} w_k \left( \sum_{j=1}^{N} \frac{\partial \varphi_j\left(\frac{1}{2}(x_k+1)\right)}{\partial x} u_j \right)^2, \tag{34}$$

where $w_k$ and $x_k$ are Gaussian coefficients and Gaussian points, respectively. To overcome the part of nonlinearity terms, we adopt a predictor-corrector scheme as follows. We rewrite Eqs. (31)-(33) in the matrix form as follows:

$$A U^{n+1} = \rho_n B U^n + b, \tag{35}$$

where

$$\rho_n = \frac{1}{2} \sum_{k=1}^{n} w_k \left( \sum_{j=1}^{N} \frac{\partial \varphi_j\left(\frac{1}{2}(x_k+1)\right)}{\partial x} u_j^n \right)^2$$

and matrices $A, B$ and vector $b$ are defined as follows:

$$A_{ij} = \begin{cases} D^{(4)}_{x_{ij}}, & i = 1,2,...,N_\Omega - 2 \\ \delta_{ij}, & i = 1, N \\ D^{(1)}_{x_{ij}}, & i = 2, N-1 \end{cases}, \quad j = 1,2,...,N, \tag{36}$$

$$B_{ij} = \begin{cases} D^{(2)}_{x_{ij}}, & i = 1,2,...,N_\Omega - 2 \\ 0, & i = 1,2, N-1, N \end{cases}, \quad j = 1,2,...,N, \tag{37}$$

$$b_i = \begin{cases} -\frac{\alpha}{(u_i^n)^\zeta} - \frac{\beta}{(\kappa + u_i^n)^2} - \frac{\gamma}{u_i^n}, & i = 1,2,...,N_\Omega - 2, \\ 1, & i = 1, N, \\ 0, & i = 2, N-1 \end{cases}, \tag{38}$$

$$U^n = (u_1^n, u_2^n, ..., u_N^n)^{tr}, \quad U^n = (1,1,...,1)^{tr}. \tag{39}$$

In Eqs. (36) and (37), $\delta_{ij}$ is obviously the Kronecker delta function, i.e.

$$\delta_{ij} = \begin{cases} 1 & , i = j \\ 0 & , i \neq j \end{cases}. \tag{40}$$

*Numerical Experiments and Comparison*

In this section, we show the results obtained for some case studies which have been adopted from Ref. [18] using the SMRPI method described in previous sections. In these examples, $N$, the number of total nodal points covering $\Omega$, is regularly distributed. Also in order to implement the SMRPI method, the radius of support domain (that is a interval in one dimension) to construct basis functions is chosen $r_s = 4.2h$, where $h$ is the distance between the nodes in $x$ direction. Also, the integrals (34) are evaluated with $n = 8$ points Gaussian quadrature rule. The obtained solutions can be compared to those of Ref. [18] and references therein. All approximate solutions reported here obtained in 1-5 seconds by Matlab softwares programm, therefore the method is highly robust.

As first case study, consider $P = \alpha = \kappa = \gamma = 0$, $\eta = 10$. The maximum deflection i.e. $1 - u(0.5)$ versus the parameter $\beta$ has been plotted in Fig. 1. In the same case, some approximate solutions (i.e. deflection of beam versus the length of beam) have been shown in Fig. 2. For the second case study, suppose $P = 0$, $\alpha = 20$, $\kappa = -0.396$, $\gamma = 0.325$, $\zeta = 4$, $\beta = 5$ and $\eta = 0.96$, the approximate SMRPI solution is seen in Fig. 3.

To validate our results, consider the boundary value problem (1)-(2) and set $\alpha = \beta = \gamma = 0$ then it leads to

$$\frac{\mathrm{d}^4 u}{\mathrm{d}x^4} - \left( \eta \int_0^1 \left( \frac{\mathrm{d}u}{\mathrm{d}x} \right)^2 \mathrm{d}x + P \right) \frac{\mathrm{d}^2 u}{\mathrm{d}x^2} = 0, \quad (41)$$

$$u(0) = u(1) = 1, u'(0) = u'(1) = 0. \quad (42)$$

It is easy to see that the unique solution to the above equations is $u(x) \equiv 1$. This point is in full agreement with our approximation result shown in Fig. 2 when $\beta = 0$. For the case the parameters are not zero, our results are comparable to those results obtained by ADM in [18].

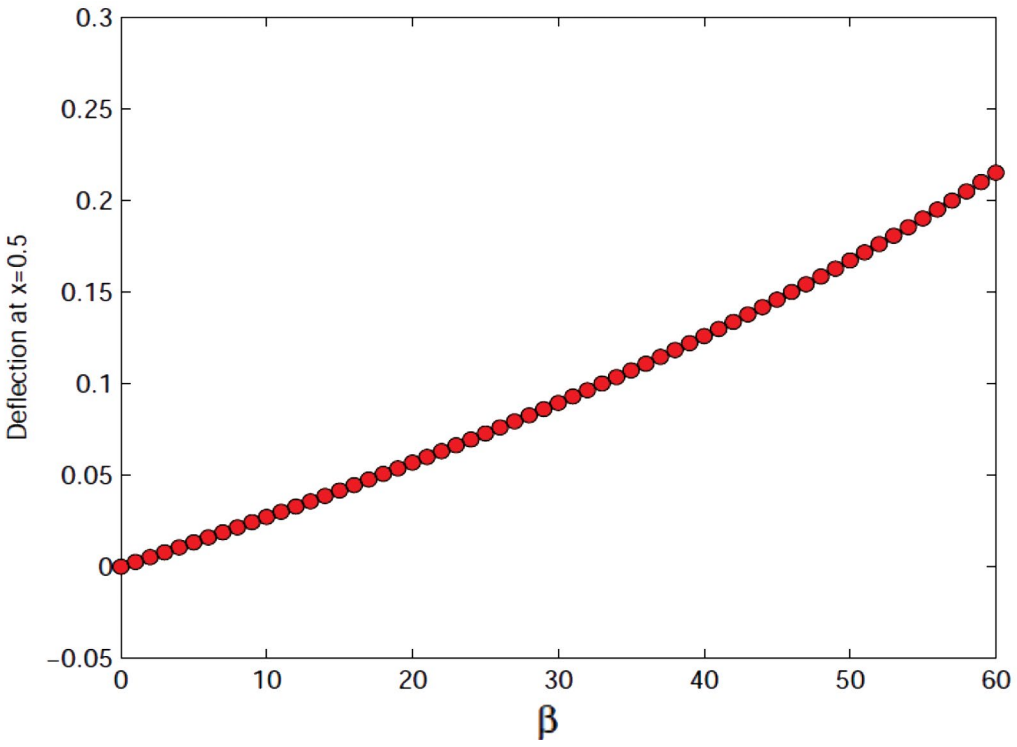


Fig. 1. The maximum deflection via $\beta$ with $N$=100.

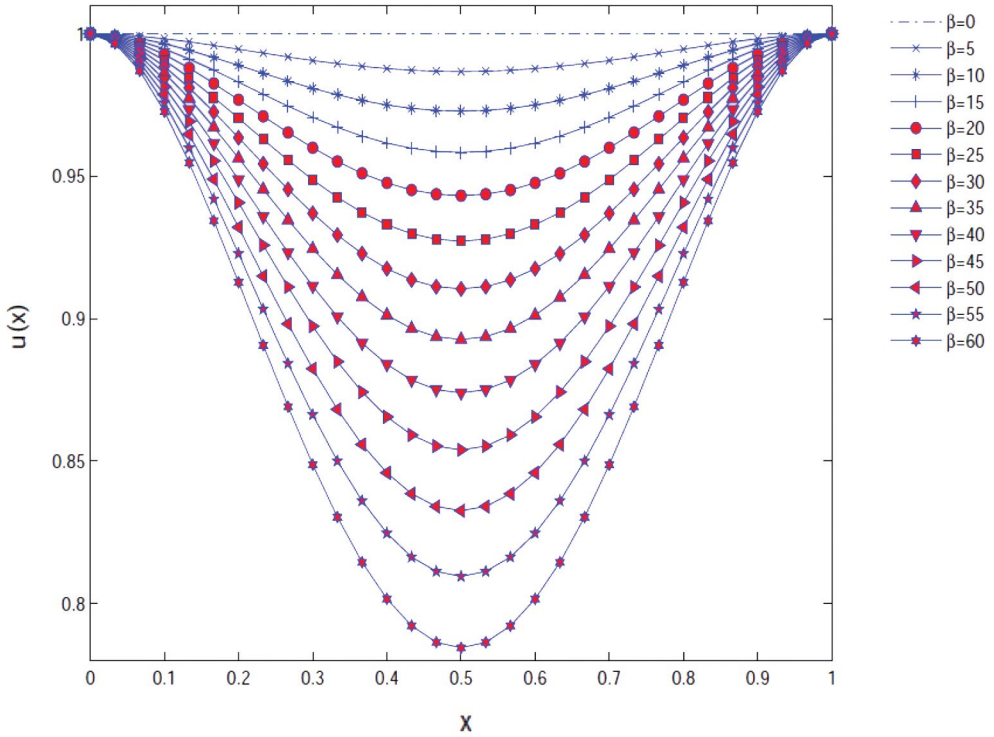


Fig. 2. The approximate solutions for different $\beta$ with $N$=30.

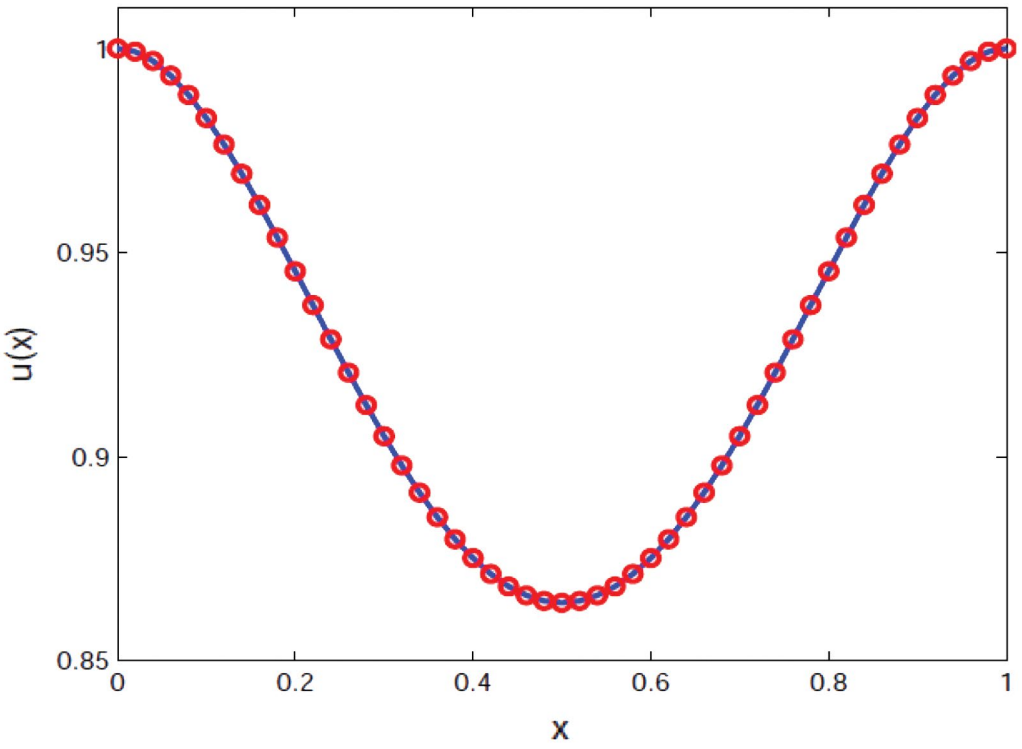


Fig. 3. The approximate solutions with $N$=50.

## CONCLUSION

The governing differential equation of clamped-clamped nano-actuators has been considered in a general form, in which the nano-actuators are subject to different nonlinear forces such as the van der Waals force, Casimir force, applied voltage, fringing field effect, capillary effect and the dielectric layer effect. Moreover, there is a nonlinear integral term in the governing equation of the nano-actuator due to the presence of the axial loads. A new spectral meshless radial point interpolation (SMRPI) method has been proposed and applied to the mentioned boundary value problem. The present method is based on meshless methods and benefits from spectral collocation techniques. The interpolation with the help of conditionally positive definite radial basis functions has been used to construct shape (basis) functions which have Kronecker delta function property. The method does not need any domain element and so it is independent of the geometry of the domain. It has been revealed through test studies that the method is highly robust and reliable.

## ACKNOWLEDGMENT

The authors are grateful to anonymous reviewers for carefully reading this paper and for their comments and suggestions which have improved the paper.

## CONFLICT OF INTEREST

The authors declare that there is no conflict of interests regarding the publication of this manuscript.

## REFERENCES

1. S. Abbasbandy, H. Roohani Ghehsareh, I. Hashim, and A Alsaedi. Engineering Analysis with Boundary Elements, 47:10–20, 2014.
2. B. Abbasnejad, Gh. Rezazadeh, and Rasool Shabani. Acta Mechanica Solida Sinica, 26(4):427–440, 2013.
3. E.M. Abdel-Rahman, M.I. Younis, and A.H. Nayfeh. Journal of Micromechanics and Microengineering, 12(6):759, 2002.
4. G. Adomian. Solving frontier problems of physics: the decomposition method, volume 60. Springer Science & Business Media, 2013.
5. R. Ansari, R. Gholami, M. Faghih Shojaei, V. Mohammadi, and S. Sahmani. Acta Astronautica, 102:140 150, 2014.
6. Mohammad Aslefallah and Elyas Shivanian. The European Physical Journal Plus, 130(3):1–9, 2015.
7. Z. Avazzadeh, V.R. Hosseini, and W Chen. Iranian Journal of Science and Technology (Sciences), 38(3):205–212, 2014.
8. W Chen, Z-J Fu, and C-S Chen. Recent advances in radial basis function collocation methods. Springer, 2014.
9. B. Choi and EG Lovell. Journal of Micromechanics and Microengineering, 7(1):24, 1997.
10. M. Dehghan and A. Ghesmati. Computer Physics Communications, 181(4):772–786, 2010.
11. M. Dehghan and D. Mirzaei. Applied Numerical Mathematics, 59(5):1043–1058, 2009.
12. GE Fasshauer and H Wendland. Scattered data approximation, 2006.
13. A. Fili, A. Naji, and Y. Duan. Journal of Computational and Applied Mathematics, 234(8):2456–2468, 2010.
14. B. Fornberg and N. Flyer. A primer on radial basis functions with applications to the geosciences, volume 87. SIAM, 2015.
15. B. Fornberg and N. Flyer. Acta Numerica, 24:215–258, 2015.
16. Bai Fu-Nong, Li Dong-Ming, W. Jian-Fei, and Cheng Yu-Min. Chinese Physics B, 21(2):020204, 2012.
17. Y Gerson, I Sokolov, T Nachmias, BR Ilic, S Lulinsky, and S Krylov. Sensors and Actuators A: Physical, 199:227–235, 2013.
18. M. Ghalambaz, M. Ghalambaz, and Mohammad Edalatifar. Applied Mathematical Modelling, 40(15):7293–7302, 2016.
19. V.R. Hosseini, W. Chen, and Z. Avazzadeh. Engineering Analysis with Boundary Elements, 38:31–39, 2014.
20. V. R. Hosseini, E. Shivanian, and W. Chen. The European Physical Journal Plus, 130(2):1–21, 2015.
21. V. R. Hosseini, E. Shivanian, and W. Chen. Journal of Computational Physics, 312:307–332, 2016.
22. YC Jiao, Y. Yamamoto, C. Dang, and Y. Hao. Computers & Mathematics with Applications, 43(6-7):783–798, 2002.
23. A. Koochi, H. Hosseini-Toudeshky, H.R. Ovesy, and Mohamadreza Abadyan. International Journal of Structural Stability and Dynamics, 13(04):1250072, 2013.
24. A. Koochi, A. Kazemi, F. Khandani, and M. Abadyan. Physica Scripta, 85(3):035804, 2012.
25. A. Koochi, A. Sadat Kazemi, Y. Tadi Beni, A. Yekrangi, and M. Abadyan. Physica E: Low-dimensional Systems and Nanostructures, 43(2):625–632, 2010.
26. J-H Kuang and C-J Chen. Mathematical and computer modelling, 41(13):1479–1491, 2005.
27. S. Liao. Homotopy analysis method in nonlinear differential equations. Springer, 2012.
28. B Nayroles, G Touzot, and P Villon. Computational mechanics, 10(5):307–318, 1992.
29. A. Noghrehabadi, M. Ghalambaz, and Afshin Ghanbarzadeh. Computers & Mathematics with Applications, 64(9):2806–2815, 2012.
30. M. Peng, D. Li, and Y. Cheng. Engineering Structures, 33(1):127–135, 2011.
31. A Shirzadi and F Takhtabnoos. Inverse Problems in Science and Engineering, 24(5):729–743, 2016.
32. E. Shivanian, S. Abbasbandy, M.S. Alhuthali, and H.H. Alsulami. Engineering Analysis with Boundary Elements, 56:98–105, 2015.
33. E. Shivanian. Engineering Analysis with Boundary Elements, 37(12):1693–1702, 2013.
34. E. Shivanian. Engineering Analysis with Boundary Elements, 54:1–12, 2015.
35. E. Shivanian. International Journal for Numerical Methods in Engineering, 105(2):83–110, 2016.
36. E. Shivanian and A. Jafarabadi. Engineering Analysis with Boundary Elements, 72:42–54, 2016.
37. E. Shivanian and HR Khodabandehlo. Ain Shams Engineering Journal, 2015.
38. E. Shivanian. Engineering Analysis with Boundary Elements, 50:249–257, 2015.
39. R. Soroush, A. Koochi, A. Sadat Kazemi, and M. Abadyan. International Journal of Structural Stability and Dynamics, 12(05):1250036, 2012.
40. A. Tadeu, CS Chen, J. António, and N. Simoes. Advances in Applied Mathematics and Mechanics, 3(05):572–585, 2011.
41. A-M Wazwaz. Applied Mathematics and Computation, 161(2):543–560, 2005.
42. E. Yazdanpanahi, A. Noghrehabadi, and M. Ghalambaz. International Journal of Non-Linear Mechanics, 58:128–138, 2014.